## Chapter 2 – Extrinsic Fabry-Perot Interferometer Measuring Magnetic Field

The Fabry-Perot interferometer consists of two parallel reflectors separated by a fixed distance. A monochromatic optical wave incident upon an etalon at an arbitrary angle to the normal of the mirror (semi transparent reflector) will experience multiple reflections within the mirrors. The intensity distribution of the reflected and refracted interfering beams using an etalon generates a set of fringes for each case. The distance of interfering peak or bottom of the fringe is dependent on the spacing between the etalon mirrors and the inverse wavelength of the light. Hence, the basic function of the F-P interferometer is to transform wavelength into an displacement. The main advantages of F-P interferometers based on optical fiber over the other sensor configurations such as Michelson, Mach-Zehnder, and Sagnac interferometers are lightness and compactness, high reliability, low cost, and ease in fabrication. Hence optical fiber based Fabry-Perot (F-P) sensors have been used for measuring temperature, strain, vibration, acoustic waves, and magnetic fields. The measurement of voltage and pressure were done by using an etalon based F-P configuration [2.1]. Beside this classic etalon based configuration, there are several ways to fabricate the Fabry-Perot cavity such as using Bragg gratings in or on the fiber [2.2], and air-glass interfaces at the fiber ends as the reflectors [2.3]. An etalon sensor was fabricated in a continuous length of fiber by a pair of semireflective splices [2.4]. In this case, the optical wave resides inside the fiber so that the sensing mechanism is intrinsic. The F-P sensors based on air-glass reflectors are referred to as the extrinsic F-P interferometers (EFPI). The extrinsic Fabry-Perot interferometer does not have the polarization rotation problem which is inherent in intrinsic F-P interferometer since the light leaves air-glass interface and reflected back through the air gap between the reflectors. Hence the EFPI configuration is suitable for measuring a low exturbance.

### 2.1 Principle of the Basic EFPI Sensor

A typical EFPI sensor configuration is shown in Figure 2.1. The light from a laser source propagates along an input/output single mode fiber to the Fabry-Perot cavity that is formed by the input/output and the target fibers. A fraction of this incident light, approximately 4 %, is reflected at the output endface of the input/output fiber back into the fiber. The light transmitted out of the input/output fiber projects onto the fiber endface of the target fiber. The reflected light from the target fiber is partially recoupled into the input/output fiber. The interference between the two reflections produces interfering fringes as the air-gap is changed.

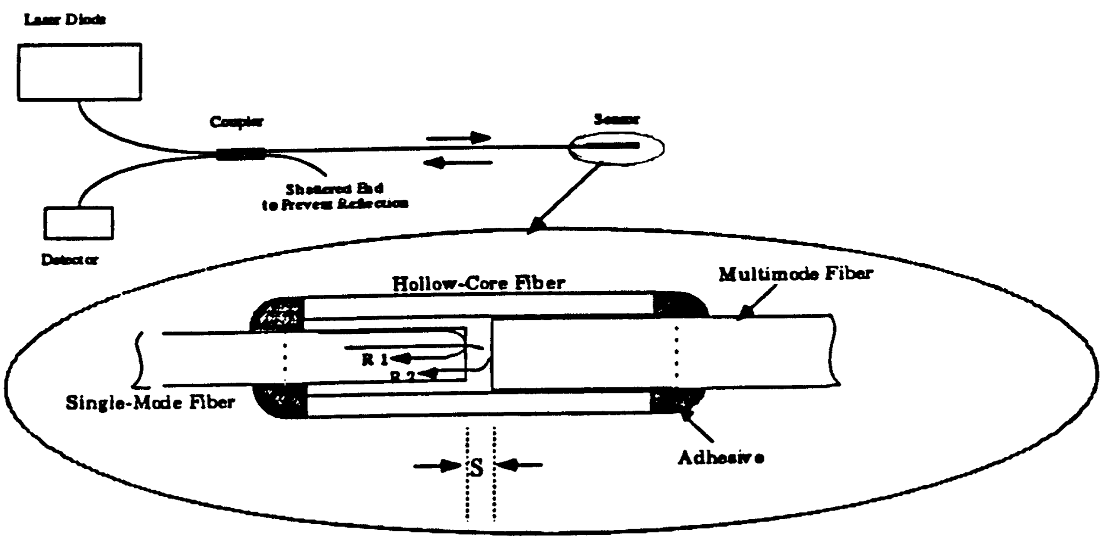


Figure 2.1 Typical EFPI sensor structure.

The optical wave fields of the two reflections could be represented in terms of its complex amplitude $U_i(x,z,t)$ given by

$$U_i(x,z,t)=A_i exp(j\phi_i),\ i=1,2 \tag{2.1}$$

where the variable $A_i$ is a function of the transverse coordinate $x$ and traveled distance $z$, and the subscripts $i$= 1,2 stand for the reference and sensing reflections, respectively. Assuming that the reference reflection $A_1=A$, then the sensing reflection coefficient $A_2$ can be approximated by the simplified relation

$$A_2 = A[\frac{ta}{a + 2s\,tan[sin^{-1}(NA)]}] \quad (2.2)$$

where $a$ is the fiber core radius, $t$ is the transmission coefficient of the air-glass interface(≈0.98), $s$ is the separation between the reflectors, and $NA$ is the numerical aperture of the single mode fiber given as $NA = (n_1^2 - n_2^2)^{\frac{1}{2}}$, and $n_1$ and $n_2$ are the refractive indices of the core and the cladding, respectively. The intensity detected at the photodiode is given as

$$I = |U_1 + U_2|^2 = A_1^2 + A_2^2 + 2A_1A_2cos(\phi_1 - \phi_2) \quad (2.3)$$

which can be expanded as

$$I = A^2[1 + \frac{2ta}{a + 2s\,tan[sin^{-1}(NA)]}cos(\frac{4\pi s}{\lambda}) + (\frac{ta}{a + 2s\,tan[sin^{-1}(NA)]})^2] \quad (2.4)$$

we have assumed that $\phi_1 = 0$ and $\phi_2 = 2s(2\pi / \lambda)$, and $\lambda$ is the wavelength in free space. Equation (2.4) indicates that changes in the separation distance between the surfaces of the fibers aligned in the support tube produce a sinusoidal modulation of the output signal.

## 2.2 Basic Sensor Design

A preliminary fiber magnetic field sensor based on the basic EFPI configuration was designed to evaluate candidate magnetostrictive materials. A 1300 nm single mode laser was used as the source. The pure EFPI sensors was attached to a Metglas ribbon or Terfenol-D rod by using epoxy, and magnetic fields were applied to evaluate the magnetostrictive properties of each material. Since only ribbon type Metglas was available at the initial stage of the research, the basic sensor design at that stage seems logical. The schematic of the sensor is given in Figure 2.2.

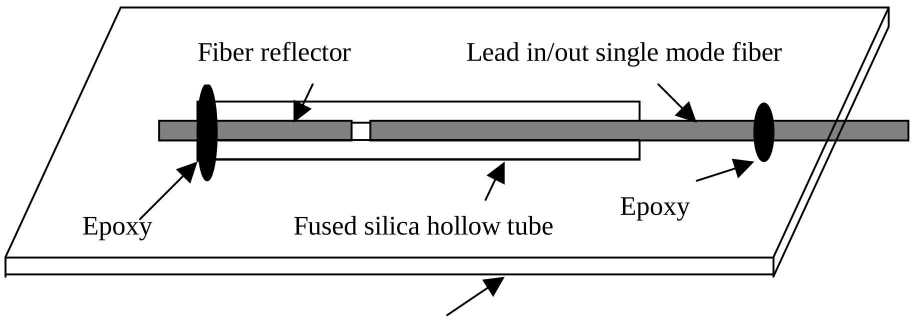


Figure 2.2 Basic sensor design used to evaluate magnetostrictive characteristics of candidate materials.

## 2.3 Magnetic Properties of Ferromagnetic Materials

The binary or pseudobinary compounds of the rare earth-$Fe_2$ ($RFe_2$) have large magnetostriction and magnetic anisotropies at room temperature. They also have relatively high magnetic saturation and Curie temperature. These characteristics are useful in realizing magnetostrictive transducers, micro positioning devices, and permanent magnets. The magnetostriction for such materials can be expressed as [2.5]

$$\varepsilon = CH^2 \tag{2.5}$$

where $C$ is $3\lambda_s/2H_A^2$, $H$ is applied magnetic field intensity, $\lambda_s$ is saturation magnetostriction, and $H_A$ is anisotropy field. As magnetic field sensing element the materials should have large magnetic saturation and smaller anisotropy field. There is a field in a ferromagnetic material which directs the magnetization along certain definite crystallographic axes called directions of easy magnetization. This field is called anisotropy field. The rare earth compound $TbFe_2$ shows large magnetostriction, more than 2000 ppm with 25 kOe field strength, at room temperature but saturated above the field strength, while the compound $DyFe_2$ relatively shows small magnetostriction, about 700 ppm at the same field strength, but hardly be saturated [2.6]. The proper control of each element mole fraction could yield maximum magnetostriction and high saturation magnetostriction value. The pseudobinary compound $Tb_xDy_{1-x}Fe_2$ ($0<x<1$) exhibits a maximum magnetostriction / anisotropy ratio at $x \cong 0.3$ with 25kOe [2.6]. Figure 2.3 shows the room temperature measurement of a strain which is strain parallel to the magnetic field minus strain perpendicular to magnetic field applied as a function of x. This ternary compound is commercially available under the trade name Terfenol.

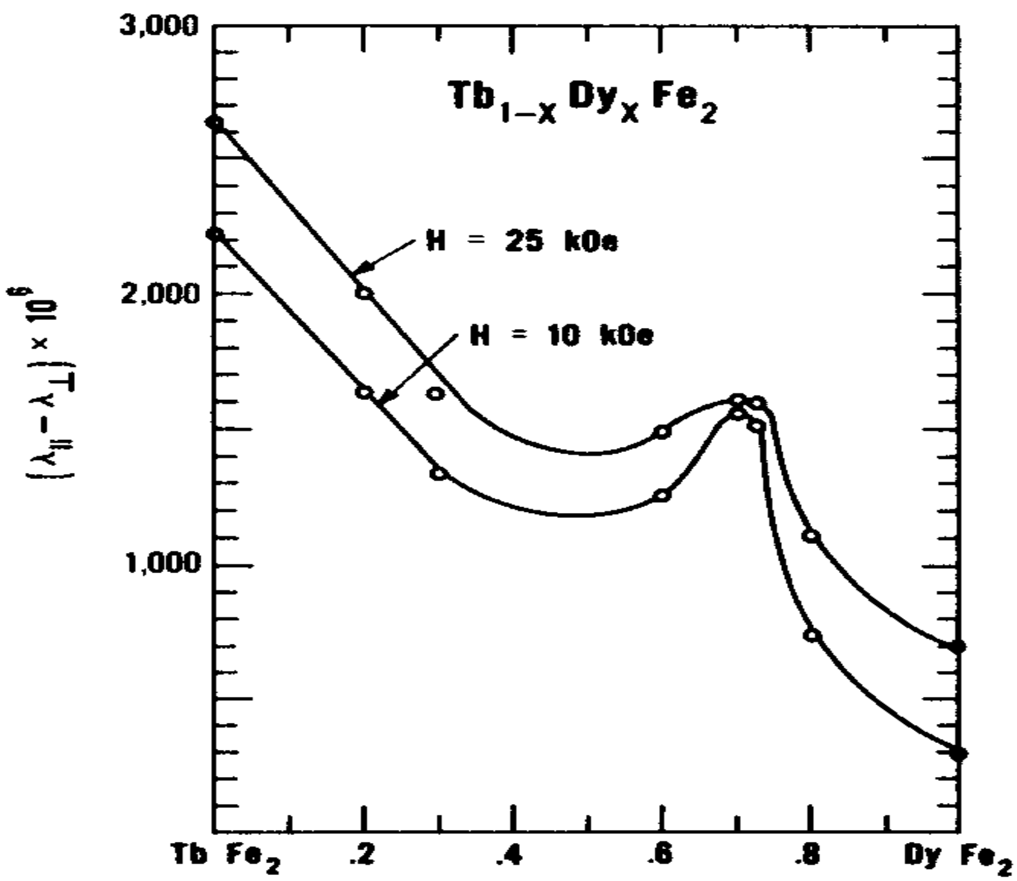


Figure 2.3 Magnetostriction of $Tb_{1-x}Dy_xFe_2$ as a function of x [2.6].

The other ferromagnetic material sets a group of high magnetostrictive materials based on silica amorphous polycrystalline. Glasses are used and well-known as with hardness, brittleness, and transparency of typical window materials which are made up mostly of silica and oxides of metals such as Al, Ca, K, Mg, and Na. The transition from the liquid to solid state is progressive and the viscosity of the melt increases with decreasing temperature. The eventual shear viscosity rises to be considered as solid for practical purposes. During this progressive transition from liquid to the solid state, the atoms do not form the regular crystalline structure but instead remain locally defined structure. Hence the atomic arrangement of a glass is similar to that of liquid with the same composition. Metallic glasses, obtained by rapid quenching of metallic melts, are also non-crystalline or amorphous, like glasses, but also are different to the latter in several aspects. They are primarily composed of metallic elements and the bondings between the molecules are metallic in nature. They are usually opaque, not brittle but their physical, chemical, and mechanical properties are similar to those of traditional metallic materials, or even superior to those of their crystalline counterparts. Amorphous metals and alloys can be produced by several techniques such as the rapid solidification of metallic melts, vapor deposition, sputtering, electrodeposition, and irradiation. But the term used as metallic glass currently represents the material with reference to foils, powders, ribbons, tapes, wires, and strips which are obtained by rapid solidification process of alloy melts. The alloy melts are cooled through the specific temperature range, within which solidification or crystallization would normally occur at rates of between $10^5$ and $10^8$ K/s [2.7]. The metallic glasses show soft magnetic properties, which refers to the fact that the response of the magnetization to the applied field is large. For the magnetization to change in large in value for a small applied magnetic field usually shows weakly coupled magnetization to the material. The material possesses a low magnetic anisotropy so that the magnetic moments are easily rotated by applied field at room temperature.

## 2.4 Investigation of Magnetostrictive Characteristics

Two candidate magnetostrictive materials were evaluated for the design and fabrication of the magnetic field sensors. According to the survey, Terfenol-D and Metglas are the two most commonly used magnetostrictive materials for magnetic field sensing. To test the linear range and sensitivity of the selected materials, a basic EFPI sensor based testing system was constructed based on these materials. The experimental setup is shown in Figure 2.4. As shown in Figure 2.2 an EFPI sensor was attached to a Terfenol-D bar with one inch long and 6 mm in diameter. A solenoid was used to generate magnetic fields and the sensor was inserted inside the coil. The gage length of EFPI sensor was 20 mm.

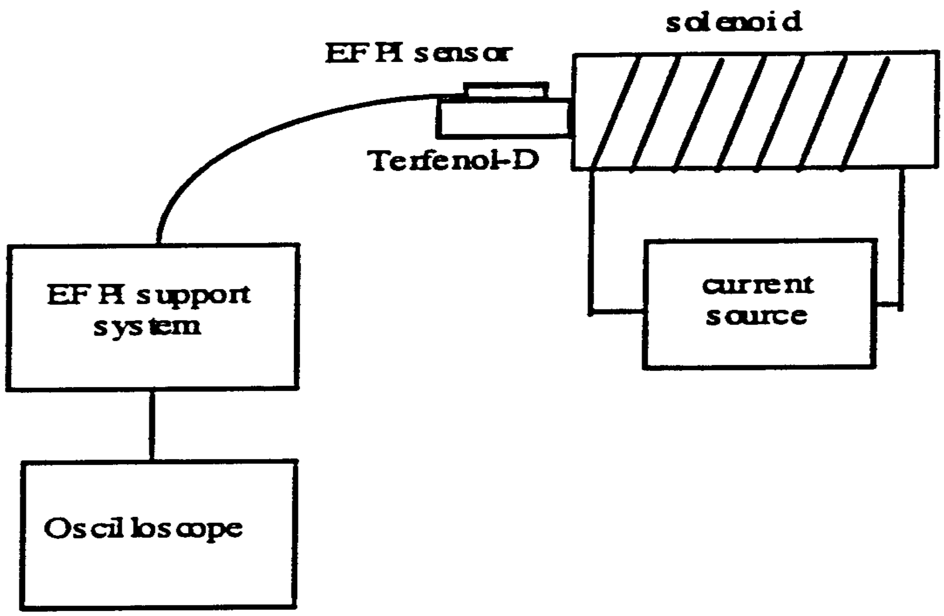


Figure 2.4 Schematic of the experimental setup used for the evaluation of candidate magnetostrictive materials.

A Gauss meter was used to monitor the magnetic field flux density and the field was increased from 0 to 600 Gauss. The dependence of the magnetic field induced strain on the applied field intensity is shown in Figure 2.5. It is obvious from the figure that the Terfenol-D is insensitive to the low magnetic field (<450 Oe), but becomes very sensitive at high field level. The magnetostriction of ternary compound $Tb_xDy_{1-x}Fe_2$ is high when the concentration of x is approximately 0.3, which is called Terfenol-D. The saturation value of 1068 ppm is achieved by Terfenol ($Tb_{0.3}Dy_{0.7}Fe_2$) at near 25 kOe [2.6]. It is observed that elongation of the Terfenol is about 500 ppm at 100 kA/m field intensity without pressure. The approximate flux density is 0.126 Tesla. In order to detect 100 nT flux density, the Terfenol should respond to 0.076 A/m field intensity. At this intensity, Terfenol gives virtually no elongation as we have seen in this experiment. Since the major objective of this dissertation research is to design and fabricate magnetometers for weak magnetic fields (range 100 nT-40,000 nT), Terfenol-D is thus not suitable for this application.

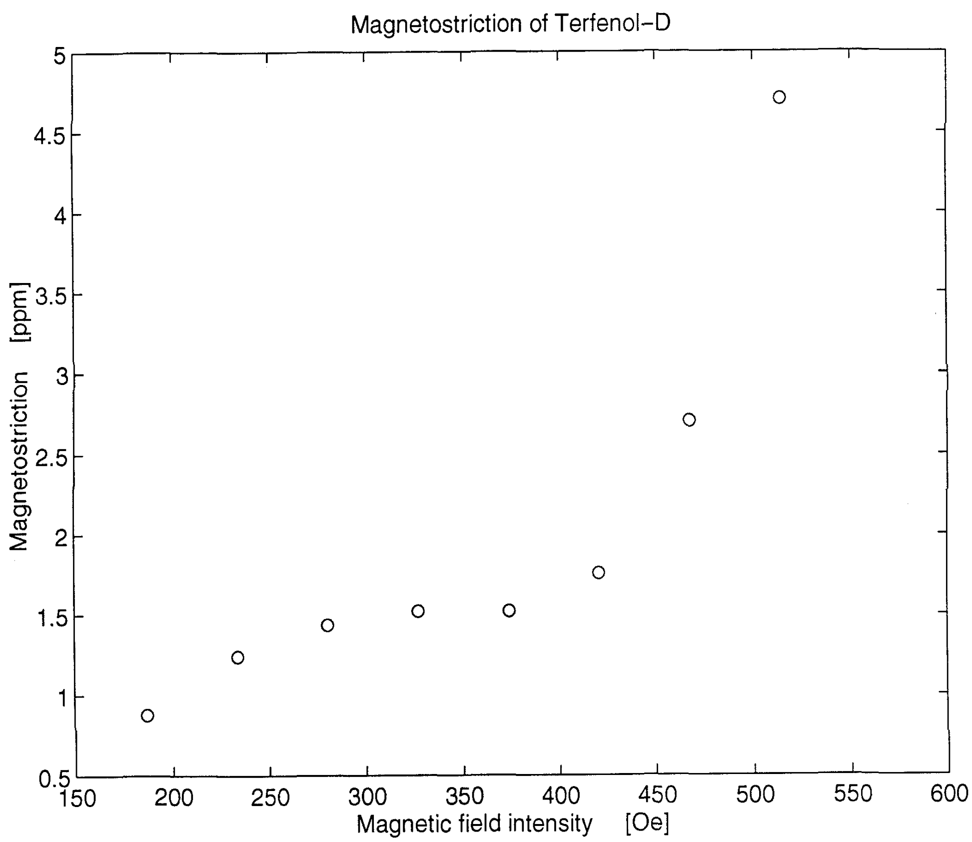


Figure 2.5 Magnetostriction as a function of magnetic field intensity for Terfenol-D.

For measuring low magnetic fields, the other material, Metglas 2605 ($Fe_{78}B_{13}Si_9$), was evaluated. A 25 mm long Metglas ribbon was used to bond with the fiber sensor to measure the magnetic field induced strain. The EFPI sensor used had a gage length of 20 mm. The sensor was attached on the Metglas ribbon with an epoxy based adhesive, and the applied field was increased from 0 to 50 Oe. The results are shown in Figure 2.6.

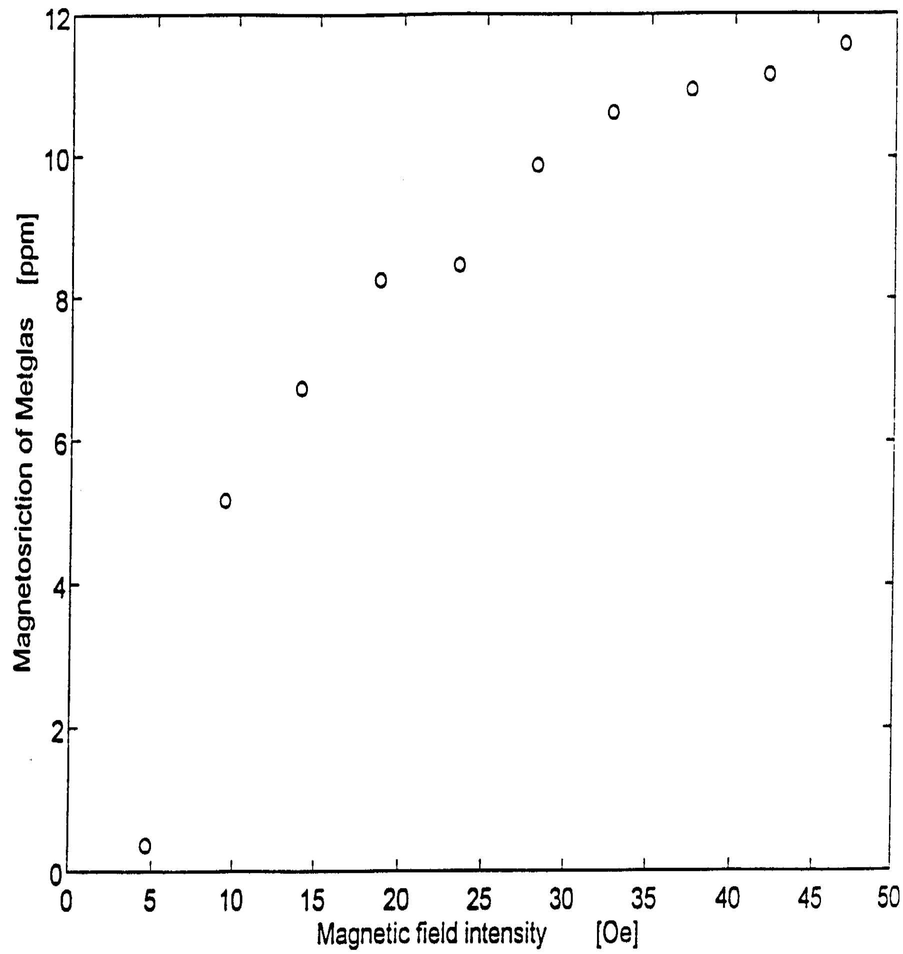


Figure 2.6 High field magnetostrictive characteristics of Metglas ($Fe_{78}B_{13}Si_9$) ribbon.

It was noted that Metgals-2605 had a small magnetostriction at both weak and strong fields but displayed high sensitivity at mid intensity of applied fields. In order to measure the linear range of magnetostriction with a higher resolution, the current to the flux coil was controlled carefully. The field was increased from 4.5 to 9.5 Oe. The results are shown in Figure 2.7. It was observed that within 5-6 Oe, the field dependence was the most linear and sensitive. Hence the sensors biased at this field level can possess maximum sensitivity to the applied magnetic fields.

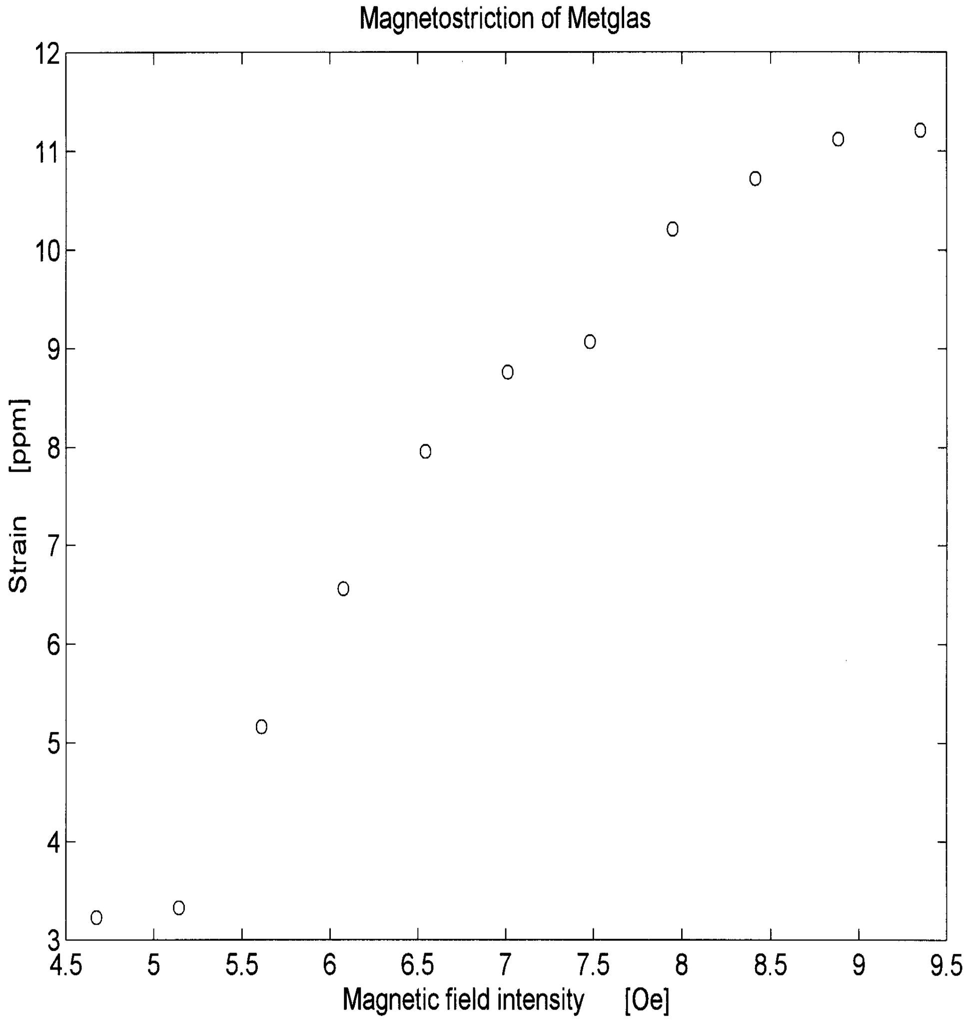


Figure 2.7 Low field magnetostrictive characteristics of Metglas ($Fe_{78}B_{13}Si_9$) ribbon.

Hence the Metglas is suitable for measuring mid to low magnetic field. The next step was to determine the minimum detectability of this material. In order to test the minimum detectable magnetic field of fabricated EFPI sensors, a 5 Hz AC current source and a small coil were used to simulate the weak magnetic fields. The solenoid was used to provide the necessary field bias (5.5 G). The sensor used had a gage length of 20 mm. The data from the oscilloscope was signal processed using a digital signal processing techniques. Both low-pass and band-pass Butterworth filters were designed to extract the applied 5 Hz signal from the noisy background. It is shown that the output signal without digital signal processing and after signal processing in Figure 2.8. The experimental results clearly demonstrate the feasibility of measuring magnetic fields with magnitude of 100 nT by the Metglas-bonded EFPI sensor elements.

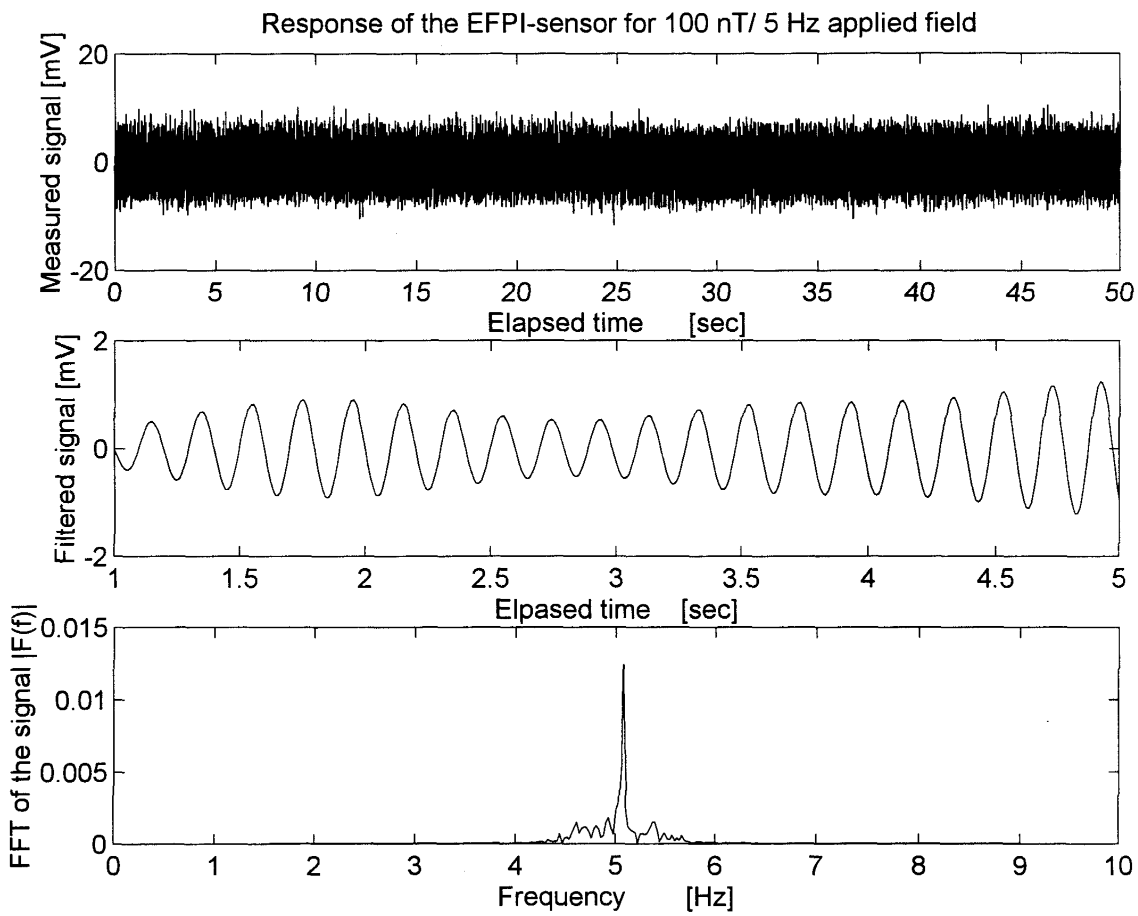


Figure 2.8 Noise reduction by a digital signal processing.

There was another type of Metglas. The shape was a wire type with a diameter of 125 μm. This format is ideal to make an EFPI sensor by insertion of this wire type Metglas into a hollow core tube. Since this Metglas wire was developed for welding applications, there is no history for using this material as a sensing element in optical fiber sensors. But the composition of this Metglas wire is $Fe_{77.5}B_{15}Si_{7.5}$, produced by Goodfellow company in UK. This is an iron based metallic glass. Hence it should have a degree of magnetostriction to external magnetic field. The evaluated magnetostriction of this material is shown Figure 2.9.

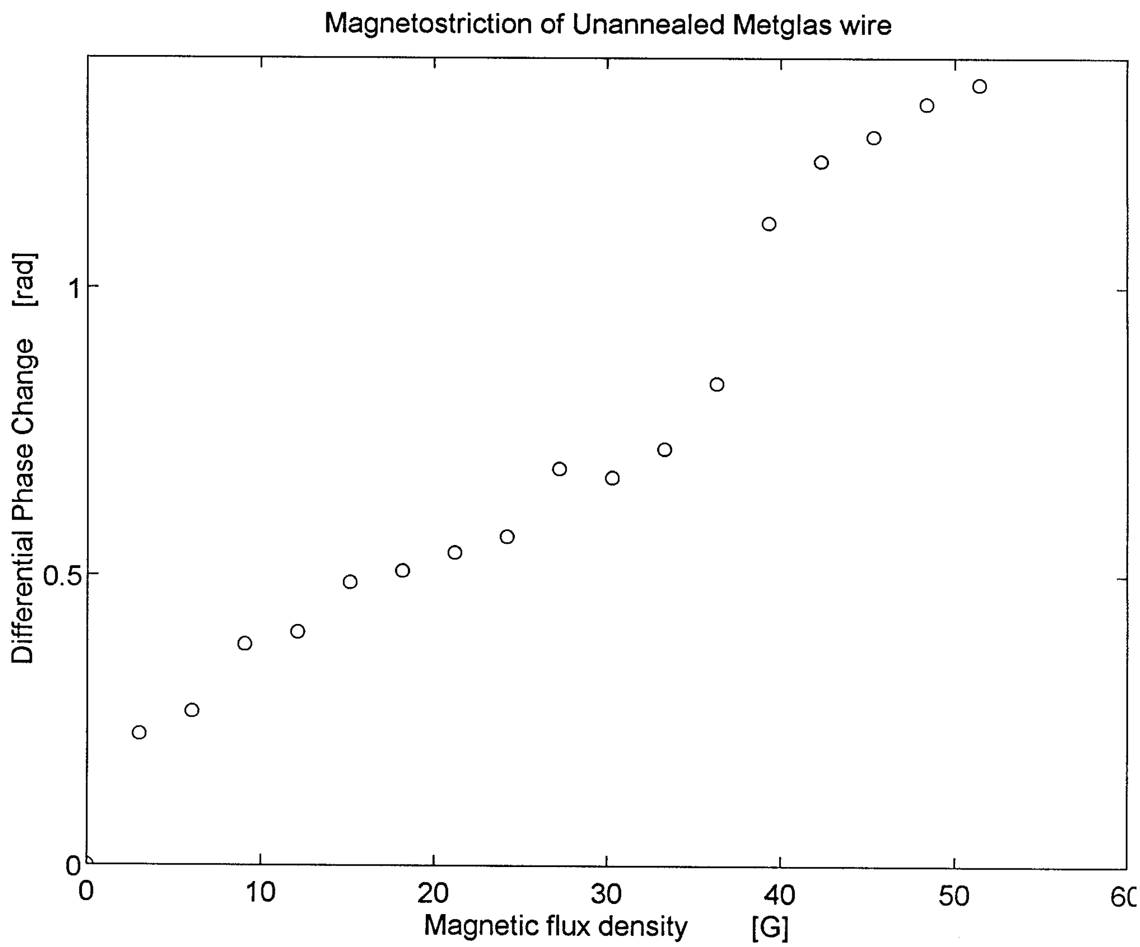


Figure 2.9 DC-magnetic field response of Metglas wire ($Fe_{77.5}B_{15}Si_{7.5}$).

### 2.5 Sensor Material Selections

The results presented in the proceeding section suggest that the Metglas materials can be used for sensor design. One shape of the Metglases was available in ribbon. Since the thickness of the ribbon was 20 μm, it was too flexible to fix the basic EFPI on it by epoxy. This is a mechanical disadvantage of the ribbon type Metglas, although magnetostrictive characteristics are suitable for our purpose. Since the Metglas ribbon was susceptible to bending and vibration, the performance of the EFPI attached onto it was severely reduced. This conventional EFPI configuration results in low magnetic field sensitivity and unreliable read out for weak magnetic field measurements.  At the same time, the shape of Metglas wire was distorted a lot and very hard to straightening so that it was impossible to insert this Metglas wire into a hollow core glass tube to make an EFPI sensor.  The technical tasks are to overcome these problems and to improve the sensor performance are discussed in the next chapter.